

## Mutational Evidence of Transition State Stabilization by Serine 88 in *Escherichia coli* Type I Signal Peptidase<sup>†,‡</sup>

Joseph L. Carlos,<sup>§</sup> Philip A. Klenotic,<sup>§</sup> Mark Paetzel,<sup>||</sup> Natalie C. J. Strynadka,<sup>||</sup> and Ross E. Dalbey<sup>\*,§</sup>

Department of Chemistry, The Ohio State University, Columbus, Ohio 43210, and Department of Biochemistry and Molecular Biology, University of British Columbia, Vancouver, British Columbia V6T 1Z3, Canada

Received February 8, 2000; Revised Manuscript Received April 6, 2000

**ABSTRACT:** Type I signal peptidase (SPase I) catalyzes the hydrolytic cleavage of the N-terminal signal peptide from translocated preproteins. SPase I belongs to a novel class of Ser proteases that utilize a Ser/Lys dyad catalytic mechanism instead of the classical Ser/His/Asp triad found in most Ser proteases. Recent X-ray crystallographic studies indicate that the backbone amide nitrogen of the catalytic Ser 90 and the hydroxyl side chain of Ser 88 might participate as H-bond donors in the transition-state oxyanion hole. In this work, contribution of the side-chain Ser 88 in *Escherichia coli* SPase I to the stabilization of the transition state was investigated through in vivo and in vitro characterizations of Ala-, Cys-, and Thr-substituted mutants. The S88T mutant maintains near-wild-type activity with the substrate pro-OmpA nuclease A. In contrast, substitution with Cys at position 88 results in more than a 740-fold reduction in activity ( $k_{\text{cat}}$ ) whereas S88A retains much less activity (>2440-fold decrease). Measurements of the kinetic constants of the individual mutant enzymes indicate that these decreases in activity are attributed mainly to decreases in  $k_{\text{cat}}$  while effects on  $K_{\text{m}}$  are minimal. Thermal inactivation and CD spectroscopic analyses indicate no global conformational perturbations of the Ser 88 mutants relative to the wild-type *E. coli* SPase I enzyme. These results provide strong evidence for the stabilization by Ser 88 of the oxyanion intermediate during catalysis by *E. coli* SPase I.

Proteins that are exported across the bacterial cell membrane generally contain amino-terminal signal peptides that are cleaved during translocation of the exported protein across the lipid bilayer. Cleavage of these signal peptides is accomplished by type I signal peptidases (SPase I).<sup>1</sup> Since these enzymes are essential for the viability of most bacteria (1–3), they are currently of interest as possible targets for the design of novel antibiotics (4).

Type I SPases identified in eubacteria and the mitochondria and chloroplasts of higher eukaryotes appear to be unconventional Ser proteases. They are classified into a novel class distinguished by a conserved Ser/Lys dyad catalytic mechanism (5). Included in this classification (Clan SF) are the LexA repressor protein, *Bacillus subtilis* SPase I (SipS), Tsp protease, and tricorner protease (6). The catalytic system employed by these endopeptidases is hypothesized to occur via the use of a Lys side chain as a general base in the deprotonation of a nucleophilic Ser residue. In contrast, the Lys general base is replaced by a His in the proposed catalytic

mechanism of SPase I enzymes found in archaea and the endoplasmic reticulum. No conserved Lys residue has been found to be necessary for catalysis in these enzymes (7).

The most direct evidence to date of the catalytic mechanism of type I signal peptidases has been provided by the crystal structure of the inhibitor-bound soluble fragment of *Escherichia coli* SPase I (8). The structure reveals the  $\beta$ -lactam type inhibitor [allyl (5S,6S)-6-[(R)-acetoxyethyl]-penem-3-carboxylate] carbonyl (C7) covalently bonded to the Ser 90 O $\gamma$ . The structure also shows that the only titratable residue in the vicinity of the nucleophilic Ser 90 side chain is Lys 145. The Lys 145 N $\zeta$ , at 2.9 Å away from the Ser 90 O $\gamma$ , is properly positioned to function as the general base during catalysis. An additional feature of the catalytic mechanism of *E. coli* SPase I revealed by the crystal structure is the likely formation of a transition-state oxyanion hole. Though the Ser 90 backbone amide group was shown to be a strong candidate to provide electrophilic assistance in the stabilization of the tetrahedral oxyanion intermediate, no other main-chain or side-chain groups were correctly positioned. However, the Ser 88 residue was a likely candidate, provided that it was rotated about its  $\chi_1$  angle to overcome steric conflicts with the bound inhibitor.

In the present study, site-directed mutagenesis of the full-length *E. coli* SPase I enzyme was used to investigate the role of Ser 88 in stabilizing the oxyanion transition-state intermediate. The Ser 88 residue is indeed involved in catalysis as demonstrated by maintenance of almost full activity by an S88T mutant but drastic reduction in activity by S88A and S88C mutants in vivo and in vitro. The changes in

<sup>†</sup> This work was supported partially by National Institutes of Health Grant GM 48805 to R.E.D. In addition, N.C.J.S. is funded by the Medical Research Council of Canada, the Canadian Bacterial Diseases Network of Excellence, and the Burroughs-Wellcome Foundation. M.P. is funded by a Medical Research Council of Canada postdoctoral fellowship, and J.L.C. is funded by an NIH predoctoral training grant (GM 08512).

<sup>‡</sup> This work is dedicated to Tracy A. Schuenemann.

\* To whom correspondence should be addressed: Tel (614) 292-2384; fax (614) 292-1532; e-mail dalbey@chemistry.ohio-state.edu.

<sup>§</sup> The Ohio State University.

<sup>||</sup> University of British Columbia.

<sup>1</sup> Abbreviation: SPase I, type I signal peptidase.

catalytic activity are shown to be mainly due to decreases in  $k_{\text{cat}}$ , while effects on  $K_m$  were found to be negligible. All three mutants displayed similar thermal stability and CD spectra compared to wild-type enzyme. Finally, the calculated differential free energy of transition-state stabilization provided by Ser 88 was calculated to be 5.2 kcal/mol. This is consistent with the loss of an oxyanion–hydroxyl interaction (9).

## EXPERIMENTAL PROCEDURES

**Bacterial Strains and Plasmids.** The *E. coli* strains BLR(DE3) and BL21(DE3) were purchased from Novagen. The *E. coli* IT41 temperature-sensitive SPase I strain was obtained from Dr. Yoshikazu Nakamura (10). The pETlep vector, expressing wild-type 6-His-tagged *E. coli* SPase I enzyme under IPTG-inducible T7 control was constructed as described in Klenotic et al. (11). The modified pET-23a vector expressing the pro-OmpA nuclease A fusion protein was a gift from Dr. Mark O. Lively.

**Site-Directed Mutagenesis and DNA Manipulations.** Oligonucleotide PCR-directed mutagenesis was performed on the pETlep vector using the Quikchange system (Stratagene). Plasmid isolations were carried out with the Qiagen midiprep kit and plasmid DNA sequencing was accomplished by the dideoxy chain-terminator method (12) with the Sequenase 2.0 derivative of T7 DNA polymerase (U.S. Biochemical Corp.) or by the fluorescent dye termination method (ABI Prism AmpliTaq FS dye terminator cycle sequencing kit) on a Perkin-Elmer/Applied Biosystems model 373A automated DNA sequencer at The Ohio State University Biopolymer Facility. Sequencing primers were purchased from Integrated DNA Technologies. *E. coli* host strain BLR(DE3) was transformed with the pETlep vector, bearing the wild-type or mutant SPase I gene, by the calcium chloride method (13) and selected in 100  $\mu\text{g}/\text{mL}$  ampicillin and 12.5  $\mu\text{g}/\text{mL}$  tetracycline.

**Purification of 6-His-Tagged SPase I Ser 88 Mutants and Pro-OmpA Nuclease A Substrate.** Wild type and S88A, S88C, and S88T SPase I mutants containing a 6-His tag were purified on an anion-exchange nickel affinity chromatography system as described by Klenotic et al. (11). For pro-OmpA nuclease A, large-scale expression cultures (20 L) of *E. coli* (BLR DE3) transformed with the modified pET-23a vector expressing the pro-OmpA nuclease A fusion protein were grown in LB in two 14 L fermentors (New Brunswick Scientific) with a 1:40 back dilution of an overnight seed culture. The cells were grown at 37 °C at 10 L of air/min of aeration and 400 rpm agitation with 0.5 mL/L of medium chemical antifoam Mazu DF-60P (PPG Chemical). The culture was induced with a final IPTG concentration of 0.6 mM at a cell density of  $A_{600\text{nm}} = 0.5$  and, after an additional 4 h of growth at 37 °C, concentrated to 1.5 L on a Pellicon system (Millipore) with a 5.0 sq ft 0.2  $\mu\text{m}$  Durapore cassette. Cells were harvested by centrifugation at 5000g for 10 min at 4 °C. The pro-OmpA nuclease A was then isolated from the cell pellet as described by Chatterjee et al. (14) with slight modifications. The denaturing size-exclusion column was omitted and the final chromatographic step for purifying pro-OmpA nuclease A protein was an SP-Sepharose (Pharmacia) ion-exchange procedure.

**In Vitro and in Vivo Activity Assays.** The Pierce BCA protein assay kit was used to determine the concentrations

Table 1: Kinetic Parameters for the Hydrolysis of Pro-OmpA Nuclease A

| enzyme | $k_{\text{cat}}^a$ (s <sup>-1</sup> ) | $K_m^a$ ( $\mu\text{M}$ ) | $k_{\text{cat}}/K_m^a$ (M <sup>-1</sup> s <sup>-1</sup> ) | $\Delta\Delta G^\ddagger^b$ (kcal/mol) |
|--------|---------------------------------------|---------------------------|-----------------------------------------------------------|----------------------------------------|
| WT     | 44 ± 9                                | 19.2 ± 4.6                | (2.2 ± 0.5) × 10 <sup>6</sup>                             |                                        |
| S88A   | 0.018 ± 0.003                         | 35.7 ± 9.9                | (5.2 ± 0.5) × 10 <sup>2</sup>                             | 5.2                                    |
| S88C   | 0.059 ± 0.016                         | 25.4 ± 9.7                | (2.9 ± 1.4) × 10 <sup>3</sup>                             | 4.1                                    |
| S88T   | 11.8 ± 2.0                            | 15.3 ± 3.0                | (8.4 ± 3.2) × 10 <sup>5</sup>                             | 0.6                                    |

<sup>a</sup> Kinetic constants were determined as outlined under Experimental Procedures. <sup>b</sup>  $\Delta\Delta G^\ddagger$  values were determined from the values of  $k_{\text{cat}}/K_m$  by use of eq 1 in the text.

of purified SPase I constructs, and an  $E_{1\%}$  at 280 nm of 8.3 was used to determine the concentration pro-OmpA nuclease A (14). The in vitro activity of wild type and Ser 88 mutant *E. coli* SPase I was measured by the addition of 1  $\mu\text{L}$  of serially diluted enzyme (0.1, 0.01, 0.001, 0.0001, and 0.00001 mg/mL) to 10  $\mu\text{L}$  aliquots of substrate pro-OmpA nuclease A at a final concentration of 4  $\mu\text{M}$  in 50 mM Tris-HCl, 10 mM CaCl<sub>2</sub>, and 1% Triton X-100, pH 8.0. Each reaction was incubated at 37 °C for 20 min and then stopped by the addition of 10  $\mu\text{L}$  of 2× SDS sample buffer followed by quenching in a dry ice–ethanol bath. Processing of the preprotein substrate into its mature nuclease A form was determined by resolution the preprotein and mature forms by SDS–17.2% PAGE and then visualization by Gelcode Blue staining (Pierce). Measurement of in vivo processing of pro-OmpA substrate utilizing the IT41 system was performed as described in Klenotic et al. (11).

**Kinetic Assays.** The determination of kinetic constants was performed as outlined by Tschantz et al. (15) with modifications. Each cleavage reaction was initiated by the addition of each Ser 88 mutant SPase I enzyme to a sample containing pro-OmpA nuclease A substrate in 50 mM Tris-HCl, 10 mM CaCl<sub>2</sub>, and 1% Triton X-100, pH 8.0. The reactions were carried out at 37 °C with at least four different initial substrate concentrations. Typically 51.7, 25.9, 15.5, and 9.3  $\mu\text{M}$  reaction concentrations of substrate pro-OmpA nuclease A were used. The initial enzyme concentrations for S88A, S88C, and S88T were 0.0673, 0.00376, and 0.000043  $\mu\text{M}$ , respectively. During the course of the reaction, aliquots were removed at various times. Less than 8% processing of the substrate occurred at the longest incubation times. Reaction aliquots were stopped by the addition of 2× SDS sample buffer followed by quenching in a dry ice–ethanol bath. The pro-OmpA nuclease A and nuclease A proteins were resolved on SDS–17.2% polyacrylamide gels and stained with Gelcode Blue (Pierce). Stained precursor and cleaved substrate bands were scanned (Umax Astra 1200S) and quantified by U.S. National Institutes of Health's NIH Image software program (Macintosh v1.61, public domain at <http://rsb.info.nih.gov/nih-image>). Percent processing was determined by dividing the area of the mature protein band by the sum of the mature and precursor band areas.  $V_{\text{max}}$ ,  $K_m$ , and  $k_{\text{cat}}$  values were obtained by use of KaleidaGraph for Windows (version 3.09) with a Michaelis–Menten curve fit of the plot of  $v_i$  versus  $[s]$  via

$$v_i = (V_{\text{max}})([s]) / (K_m + [s])$$

All kinetic data gathered in Table 1 result from the average of a minimum of three separate sets of experimental data.

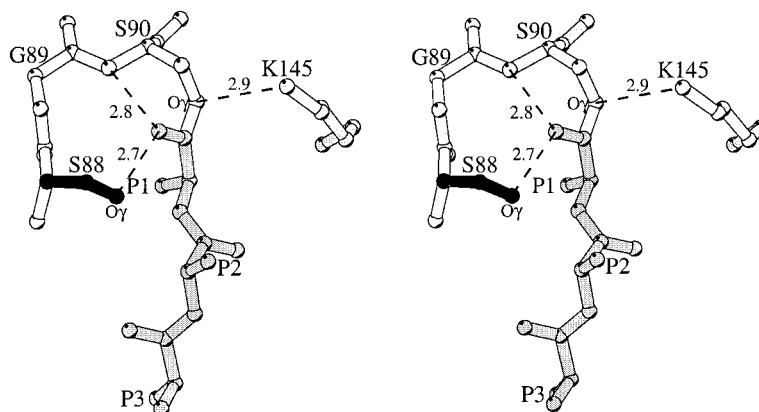


FIGURE 1: Oxyanion hole of *E. coli* signal peptidase. A signal peptidase–signal peptide acyl-enzyme complex is modeled on the basis of the crystal structure of the *E. coli* signal peptidase–inhibitor complex (8). The main-chain amide of Ser 90 and the side-chain hydroxyl of Ser 88 are the only potential hydrogen-bond donors in the environment of the substrate's scissile carbonyl oxygen. The side chain of Ser 88 is shown in black. The dashed lines indicate H-bond distances (in angstroms). The P1 through P3 residues of the substrate are shown in gray. This stereo figure was prepared with the program MOLSCRIPT (32).

**CD Spectroscopy.** The far-ultraviolet circular dichroism spectra for wild-type and Ser 88 mutant SPase I enzymes were obtained on a Jasco spectropolarimeter J-500C instrument at a constant cuvette temperature of 4 °C. As determined by use of a molar extinction coefficient of 44 000  $\text{cm}^{-1} \text{M}^{-1}$  at 280 nm (16), all protein samples were at a concentration of 10  $\mu\text{M}$  in 5 mM potassium phosphate, pH 8.0, and 1% *n*-octyl  $\beta$ -glucopyranoside detergent.

**Thermostability.** Wild-type and mutant enzymes in 20 mM potassium phosphate, pH 8.0, and 1% Triton X-100 were preincubated at the indicated temperatures for 1 h. Residual activities were then measured by the addition of 1  $\mu\text{L}$  of heat-treated enzyme to 10  $\mu\text{L}$  of substrate pro-OmpA nuclease A at a final concentration of 4  $\mu\text{M}$ . Each reaction was then incubated at 37 °C for 30 min, stopped by the addition of 2.5  $\mu\text{L}$  5 $\times$  SDS sample buffer, and quenched in a dry ice–ethanol bath. After resolution of substrate and cleavage product by SDS–17.2% PAGE and staining, percent processing was quantitated as in the kinetic assays.

**Molecular Modeling.** The program O (17) was used to perform the molecular modeling studies.

## RESULTS

The inhibitor-bound crystal structure of the soluble catalytic fragment of *E. coli* SPase I (8) showed that the Ser 90 backbone amide and the rotated Ser 88 hydroxyl side chain could participate as H-bond donors in the stabilization of a tetrahedral oxyanion intermediate during the course of catalysis. A model of these interactions with a peptide substrate is shown in Figure 1. It is clear from this model that Ser 88 may play an important catalytic role.

To confirm the role of Ser 88 in the proposed interactions, site-directed mutagenesis of full-length wild-type *E. coli* SPase I (pETlep vector) was performed to introduce Ala, Cys, and Thr at the Ser 88 position. Each mutant protein was isolated to homogeneity as previously described (11) and the expression vector DNA was sequenced to confirm the presence of each mutation.

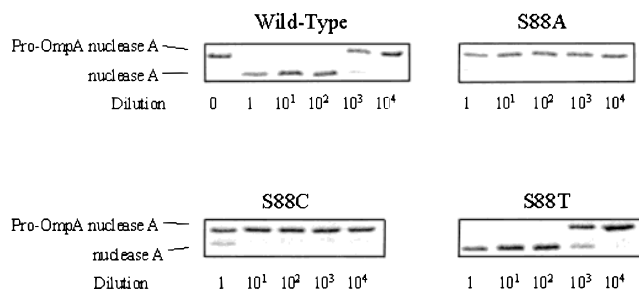
**S88T Maintains Near-Wild-Type Activity but S88A and S88C Exhibit Substantially Reduced Activity in Vivo and in Vitro.** Purified pro-OmpA–nuclease A fusion protein (14) was used as an in vitro substrate to study the *E. coli* SPase

I Ser 88 mutants. With the wild type as a control, the in vitro effects of enzyme serial dilutions on pro-OmpA–nuclease A processing were assessed for the S88A, S88C, and S88T mutants. As shown in Figure 2A, the S88A and S88C mutants displayed slight processing of the substrate at the stock 0.1 mg/mL (“1” dilution) enzyme concentration and no visible processing at 0.01 mg/mL (“10<sup>1</sup>” dilution). S88C maintains slightly greater enzymatic processing of the pro-OmpA–nuclease A substrate than the S88A mutant. Contrary to S88A and S88C, the S88T mutant exhibited processing down to a 10<sup>3</sup> stock enzyme dilution. The S88T in vitro activity was comparable to that of the wild-type enzyme.

In the temperature-sensitive SPase I-deficient IT41 strain (10), the processing of radiolabeled pro-OmpA by plasmid-encoded *E. coli* SPase I constructs can be examined in vivo. In this system, the enzymatic activities of wild-type, S88A, S88C, and S88T proteins in their native intracellular membrane environments were compared. Figure 2B shows that wild type is slightly more active than the S88T enzyme. Approximately 50% cleavage of the pro-OmpA substrate has occurred after 10 s with the S88T enzyme, whereas at the same time point greater than 50% pro-OmpA processing has already occurred with the wild-type enzyme. Also, similar to the in vitro assay results, the S88A and S88C mutants displayed very little activity in vivo. The S88A mutant showed 50% processing occurring at slightly over 40 s chase whereas the S88C mutant displayed 50% processing at slightly under 40 s (Figure 2B). The S88A and S88C SPase I activities were only slightly greater than that of the negative control cell line, which carried no plasmid encoded SPase I (Figure 2B, “no plasmid”).

**Decrease in Activity of Ser 88 SPase I Mutants Is Mainly Due to a Reduction in  $k_{\text{cat}}$ .** To determine more precisely the effects on catalysis of the Ser 88 mutations, the kinetic constants for each mutant were measured by the pro-OmpA–nuclease A in vitro assay. At constant enzyme with various substrate concentrations, initial velocities were determined from plots of pro-OmpA nuclease A processed versus time. The  $k_{\text{cat}}$  and  $K_{\text{m}}$  constants were then determined from initial velocity versus substrate concentration plots. The data are summarized in Table 1. Substitution of the hydroxyl side

A



B

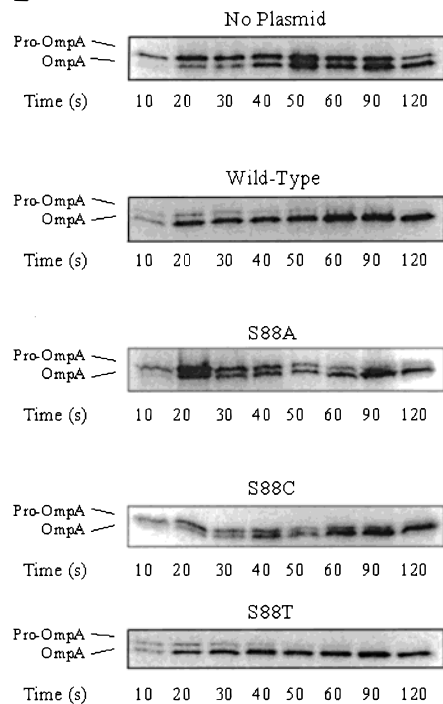


FIGURE 2: In vitro and in vivo activity of wild-type, S88A, S88C, and S88T SPase I enzymes. (A) In vitro processing of pro-OmpA nuclease A substrate by wild-type, S88A, S88C, or S88T mutant *E. coli* SPase I. Serially diluted stock enzyme, at 0.1 mg/mL ("1" dilution), of wild type or Ser 88 mutants were incubated with purified pro-OmpA–nuclease A substrate, and processing was visualized by Coomassie staining of SDS–17.2% PAGE as described under Experimental Procedures. The "0" dilution lane in the wild-type experiment indicates the control with no enzyme added. (B) In vivo processing of pro-OmpA by wild type, or S88A, S88C, or S88T mutants. Mid-log phase IT41 bearing no plasmid or pET23lep encoding wild-type or mutant Ser 88 SPase I constructs grown at 30 °C were induced with 1 mM IPTG and incubated an additional 1 h at 42 °C. After a 15 s [<sup>35</sup>S]Met pulse label, chase aliquots were removed at the indicated times and assayed for pro-OmpA processing as described under Experimental Procedures.

chain by a sulfhydryl in the S88C mutant resulted in a drastic 740-fold decrease in  $k_{cat}$ . The decrease is much more severe in the S88A mutant, displaying a 2440-fold reduction in  $k_{cat}$  compared to wild type. The S88T mutant, with a  $k_{cat}$  of 11.8 s<sup>-1</sup>, maintains approximately a quarter the activity of the native enzyme. There were only very slight effects on  $K_m$  for the S88A and S88C mutants, while the data indicate no perturbation of  $K_m$  for the S88T construct (Table 1).

For each mutant, the change in free energy of transition-state stabilization resulting from the amino acid substitutions

made at position 88 was calculated from

$$\Delta\Delta G^\ddagger = -RT \ln [(k_{cat}/K_m)^{mutant}/(k_{cat}/K_m)^{wild-type}] \quad (1)$$

The losses of transition-state binding energy for the site-directed mutants S88A, S88C, and S88T were 5.2, 4.1, and 0.62 kcal/mol, respectively.

*S88A, S88C, and S88T Mutants Maintain Similar Far-UV CD Spectra and in Vitro Thermal Inactivation Profiles.* The far-ultraviolet CD spectra of wild-type and the S88A, S88C, and S88T mutant enzymes were measured and compared. In Figure 3A, it is evident that all of the mutants exhibit similar CD spectra to that of wild-type enzyme. These data suggest no gross misfolding or changes in secondary structure of the enzymes resulting from the introduction of the mutations.

In vitro thermal inactivation profiles were also used to demonstrate that the Ser 88 mutations did not cause global conformational changes. As shown previously by Kim *et al.* (18), purified *E. coli* SPase I enzyme is stable at temperatures at or below 37 °C but can be irreversibly inactivated above 37 °C. To test for thermostability, the wild type and Ser 88 mutants were incubated for 1 h at various temperatures and then assayed for residual pro-OmpA–nuclease A processing. The wild type and S88A, S88C, and S88T mutants all displayed comparable thermostability profiles as shown in Figure 3B.

## DISCUSSION

In the studies presented here, we have shown for the first time that Ser 88 has an important catalytic role in the mechanism of *E. coli* SPase I. Amino acid substitutions of Ala or Cys at position 88 resulted in enzymes with severely impaired in vitro and in vivo catalytic activity. We propose that this is attributed to the loss of a key hydrogen-bonding interaction of the Ser hydroxyl to the tetrahedral oxyanion intermediate during the course of catalysis.

In sharp contrast to S88A and S88C, the S88T mutant displayed near-wild-type in vitro and in vivo activity (Figure 2). It is important to also point out that S88C exhibited slightly greater activity than the S88A mutant. The S88C mutant  $k_{cat}$  was approximately 3 times greater than the S88A mutant  $k_{cat}$ . In addition to the S88A, S88C, and S88T mutants presented here, we have also purified S88G and S88V mutants. The S88V and S88G mutants exhibit activity profiles similar to that of S88A (unpublished results). Molecular modeling of all mutants supports these results.

The model of a signal peptidase–signal peptide complex shown in Figure 1 allows for the Ser 88 hydroxyl side chain and the Ser 90 backbone amide to participate in the oxyanion stabilization. The distances/angles for these interactions are 2.7 Å/105° and 2.8 Å/132° for Ser 88O $\gamma$  and Ser 90N, respectively. For Ser 88O, the angle is O $\cdots$ Ser 88O $\gamma$  $\cdots$ Ser 88C $\beta$ . For Ser 90N, since the hydrogen position is unambiguous, the angle is that subtended at the calculated hydrogen position. There is a strong possibility of hydrogen bonds occurring at these contact distances and angles. On the basis of the crystal structure of the *E. coli* type I signal peptidase inhibitor complex (8), we have also modeled the active site of a signal peptidase–signal peptide complex with the various mutations at the 88 position (not shown). The modeling studies are consistent with the activity profiles. The

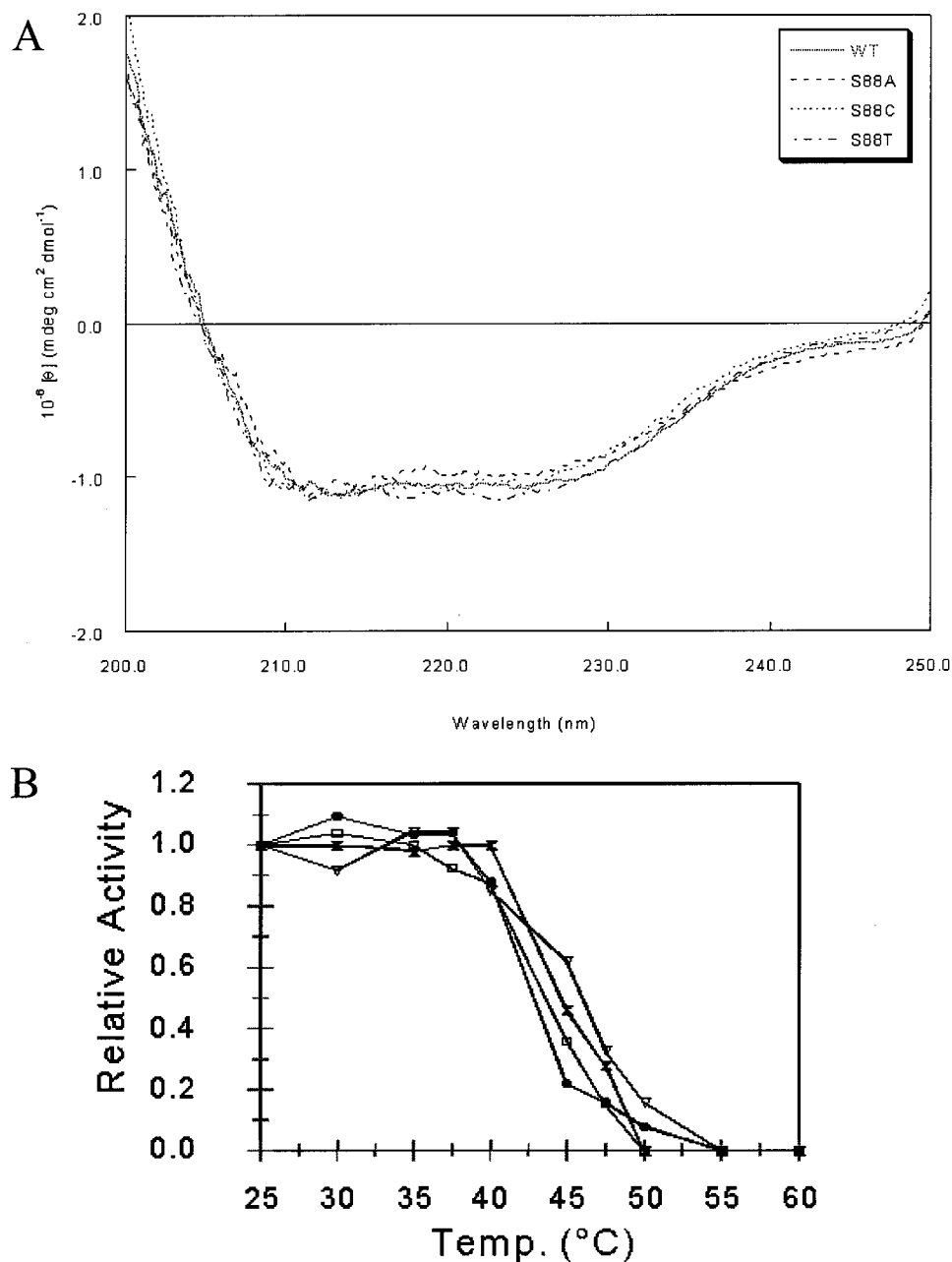


FIGURE 3: Far-UV CD spectra and thermal inactivation profiles of wild type and S88A, S88C, S88T mutants. (A) Far-UV CD spectra of wild type and S88A, S88C, S88T mutants. Each purified protein (10  $\mu$ M) was analyzed on a Jasco spectropolarimeter J-500C instrument in a 1 mm path-length cell at 4  $^{\circ}$ C. Spectra shown are an average of 5 scans/sample. (B) Thermal inactivation profiles of wild type and S88A, S88C, and S88T mutants. Each enzyme was preincubated at the indicated temperature(s) for 1 h and then assayed for residual processing of pro-OmpA nuclease A as outlined under Experimental Procedures. For each enzyme at the indicated temperature, the relative activity is calculated as the percent activity relative to activity at 25  $^{\circ}$ C. ( $\Delta$ ) Wild type; ( $\square$ ) S88A; ( $\bullet$ ) S88C; ( $\times$ ) S88T.

modeled side-chain hydroxyl group of the S88T mutant superimposes on the modeled Ser 88 hydroxyl. The side-chain methyl group on the S88T mutant points into the solvent and lies adjacent to, but does not clash with, the modeled substrate P2 side chain. In the S88C mutant, the longer  $C\beta-S\gamma$  bond distance and the larger van der Waals radius of the  $S\gamma$  results in a potential clash with the signal peptide main chain. Main-chain or side-chain adjustments may allow for the Cys 88 thiol to contribute some oxyanion stabilization and thus explain its higher activity than the S88A mutant. It should be noted that sulfur atoms are capable of forming only weak hydrogen bonds (19) and that we cannot be sure of the ionization state of the cysteine thiol group. Theoretically, at the assay reaction conditions (pH =

8.0) the thiol would be approximately 50% ionized. Modeling of the S88A mutant reveals that there would not be enough room to introduce a mediating water as a hydrogen-bond donor.

An updated model of the proposed catalytic mechanism of *E. coli* SPase I (20), which includes the transient H-bonding interactions of the transition state, is shown in Figure 4. In this scheme the amide backbone of the catalytic Ser 90 and the hydroxyl side chain of Ser 88 provide electrophilic assistance to the transition-state oxyanion. Also, the K145N $\zeta$ -scissile carbonyl oxygen distance in Figure 1 is 4.5  $\text{\AA}$ . Thus the protonated K145 residue possibly also stabilizes the oxyanion transition state through a weak Coulombic interaction (not shown in Figure 4).

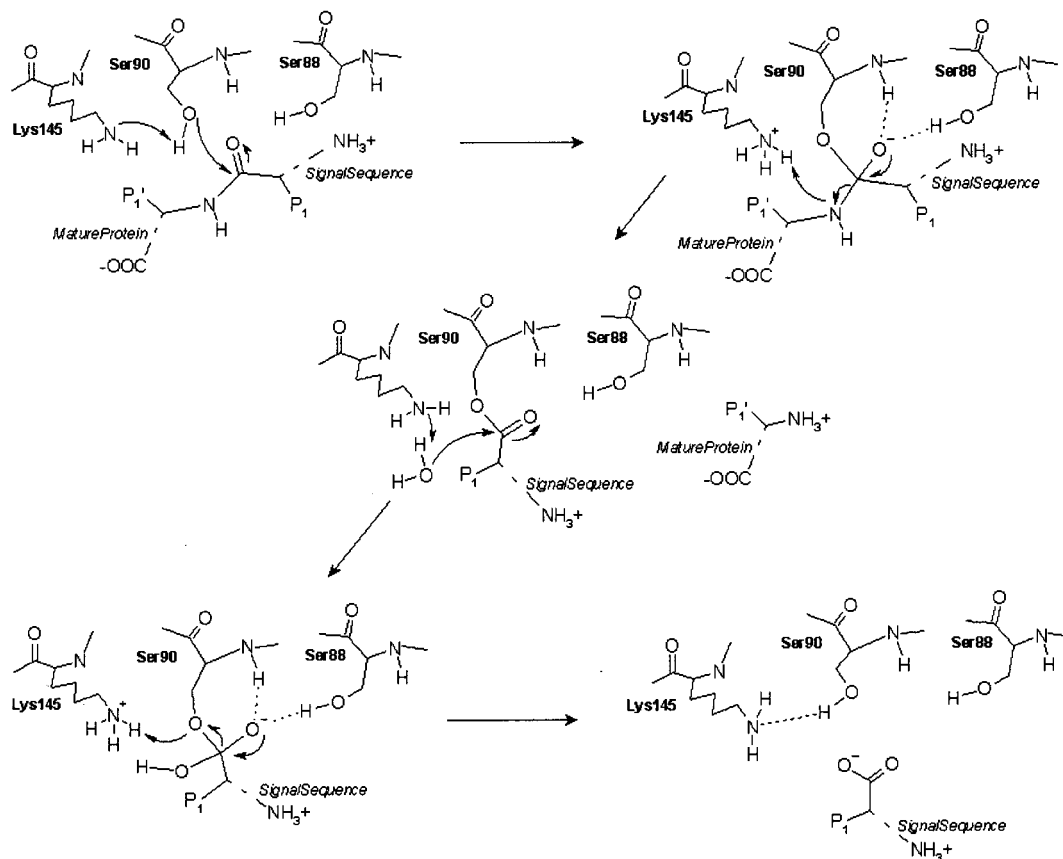


FIGURE 4: Updated proposed mechanism of *E. coli* SPase I. The proposed mechanism of Paetzel et al. (20) is updated in this scheme to include the oxyanion stabilization of the tetrahedral intermediates by the amide of Ser 90 and the hydroxyl side chain of Ser 88.

Quantitation of the kinetic constants of the *E. coli* SPase I Ser 88 mutants compared to those of wild-type enzyme shows mainly a  $k_{\text{cat}}$  rather than a  $K_{\text{m}}$  effect (Table 1). The rate-limiting step in the mechanism of *E. coli* SPase I is unknown, which precludes a straightforward interpretation of the lack of  $K_{\text{m}}$  effects with the mutants studied. If the initial acylation step is rate-limiting (Figure 4), then the data suggest that the enzyme–substrate interaction maintained by Ser 88 may not be present in the Michaelis complex. Similar results have been reported for proteases with residue-mediated oxyanion hole mechanisms such as papain (21), subtilisin (22–24), and cutinase (25). In these cases, mutation of Gln 19 of papain, Asn 155 of subtilisin, or Ser 42 in cutinase to an Ala resulted in transition-state free energy changes ( $\Delta\Delta G^\ddagger$ ,  $k_{\text{cat}}/K_{\text{m}}$ ) ranging from 2.4 to 4.2 kcal/mol, attributable mainly to a reduction in  $k_{\text{cat}}$  (25, 26). These previously reported data and those presented in Table 1 for *E. coli* SPase I are consistent with the concept of transition-state interactions in the oxyanion hole that are not present in the enzyme–substrate complex.

Type I signal peptidases can be heterogeneously subclassified as either P-type (Lys) or ER-type (His), differing according to overall amino acid conservation patterns and the conserved general base residue found in conserved region D (27). We have aligned all the currently available SPase I protein sequences from GenBank, and the results for conserved region B, containing *E. coli* S88, are presented in Figure 5. The alignment reveals that Ser, Thr, or Gly is the only residue present at the analogous *E. coli* position 88. An interesting trend is that in the P-type SPases all of the

sequences containing Gly at this position are Gram-positive bacteria (Figure 5A). Also, phylogenetic analysis [ClustalX N–J method (28–30)], unpublished results] of the aligned sequences indicates that the Gly-containing enzymes are evolutionarily distinct from those containing Ser or Thr at position 88. The Ser/Thr-containing enzymes are on separate evolutionary branches than the Gly-containing enzymes at position 88. This suggests that those enzymes with Gly at position 88 may provide backbone amide-mediated oxyanion stabilization.

In the cases of the other enzymes with a Ser or Thr at position 88, we hypothesize it is the Ser or Thr side-chain hydroxyl providing the critical transition-state interaction with the oxyanion intermediate. In support of this, site-directed mutagenesis of the analogous Ser residue (Ser 42) in the Sec11 subunit of *Saccharomyces cerevisiae* ER SPase I inhibited cell growth by 20-fold for an Ala substitution [as judged by colony size on agar plate (7)] suggesting signal peptide processing was affected. A Thr substitution at the same position did not exhibit wild-type growth as expected. Instead, the S42T mutation resulted in decreased cell growth by approximately 10-fold (7). It would be interesting to see if more direct enzyme activity experiments for these mutants in Sec11 SPase I would produce results similar to ours.

Substrate hydrolysis by classical Ser proteases, lipases, and esterases occurs through an acyl-enzyme intermediate oxyanion typically stabilized by two to three main-chain amide groups or side-chain amide or hydroxyl groups. There are examples of Ser or Thr side-chain-mediated oxyanion interactions reported for the lipase class of enzymes

| A          |            |                 |     | B          |            |                 |    |
|------------|------------|-----------------|-----|------------|------------|-----------------|----|
|            |            | *               |     |            |            | *               |    |
|            | Sip_Eco_   | PFQIPSGSMMPDLL  | 96  |            | Sip_Mth_   | HMNVVVSGSMPEPVF | 39 |
|            | Sip_Sty_   | PFQIPSGSMMPDLL  | 97  |            | Sec11_Mja_ | HVNVVVSDSMYPIM  | 23 |
|            | Sip_Hin_   | PFQIPSGSMESTLR  | 121 |            | Spc_Pho_   | PLVVVVSGSMPEPVF | 47 |
|            | Sip_Pfl_   | PFQIPSGSMKPTLD  | 96  |            | Sip_Pho_   | FVSYAYSDSMVPTI  | 43 |
|            | SipF_Bja_  | PFNIPSGSMKATLL  | 50  | Archea     | Sip_Pab_   | PLVVVASGSMRPVF  | 47 |
|            | Sip_Rca_   | PFWIPSGSMKDTLL  | 46  |            | Sec11_Afu_ | FMVAVESGSMPEHL  | 50 |
|            | Sip_Bja_   | PFVVPSSGSMPTLL  | 55  |            | Sip1_Afu_  | RLVVVSSSMPEPLM  | 41 |
|            | Sip_Mle_   | PYLIPSESMEPTLH  | 90  |            | Sip2_Afu_  | LLSYVTSDSMTPTL  | 45 |
|            | Sip_Mtu_   | PYLIPSESMEPTLH  | 102 |            | Spc21_Afu_ | RVLNTYGTSMLEPEL | 37 |
|            | Sip_Sli_   | AFVIPSGSMEQTIR  | 91  |            | Sip_Ape_   | GFAVVQGRSMPEIL  | 48 |
|            | Sip_Sco_   | PFQIPSGSMERGLR  | 83  |            |            |                 |    |
|            | Sip_Pla_   | ARYIPSESMLPTLE  | 65  | Eubacteria | SipW_Bsu_  | TLKSVLSGSMPEPEF | 52 |
|            | Sip_Ssp_   | ARYIPSSSMEPTLQ  | 58  |            | Spc21_Cpe_ | RTYSILSGSMPEPEI | 27 |
|            | Sip_Aae_   | AYTIPSASMEPTLL  | 38  |            |            |                 |    |
|            | Sip_Tpa_   | LYVIPSESMPVPSFM | 93  |            | Spc18_Ath_ | PVVVVLSGSMPEPGF | 61 |
| Eubacteria | Sip_Hpy_   | AFIIPSRSMVGTLY  | 44  |            | Sec11_Sce_ | PIVVVLSGSMPEPAF | 49 |
|            | Sip_Bbu_   | AYKIPSGSMMENTLQ | 78  |            | Sec11_Spo_ | PVVVVLSSESMEPSF | 52 |
|            | Spi_Spn_   | NVRVEGHSMPTLA   | 43  |            | Spc18_Rno_ | PIVVVLSGSMPEPAF | 61 |
|            | Sip_Smi_   | NVRVEGHSMPTLA   | 18  |            | Sip_Mmu_   | PIVVVLSGSMPEPAF | 61 |
|            | Sip_Bca_   | NYVVEGKSMPTLE   | 44  | Eucarya    | Spc18_Cfa_ | PIVVVLSGSMPEPAF | 61 |
|            | SpsB_Sau_  | PYTIKGESMDPTLK  | 42  |            | Spc21_Cfa_ | PIVVVLSGSMPEPAF | 73 |
|            | SipB_Sca_  | SYTVRGDSMYPTLK  | 42  |            | Spc18_Hsa_ | PIVVVLSGSMPEPAF | 61 |
|            | SipS_Bsu_  | PYVVDGDSMYPTLH  | 49  |            |            |                 |    |
|            | SipT_Bsu_  | PYLVEGSSMYPTLH  | 57  |            | Consensus  | p vvvlsgSMep f  |    |
|            | Sip_Bam_   | PYLVEGSSMYPTLH  | 57  |            |            |                 |    |
|            | Sip_Bli_   | PYLVEGTSMPTLH   | 50  |            |            |                 |    |
|            | SipP_pTA10 | PYVVEGKSMPTLV   | 50  |            |            |                 |    |
|            | SipP_pTA10 | PYIVQGSMKPTLF   | 49  |            |            |                 |    |
|            | SipU_Bsu_  | PFLIEGSSMAPTLK  | 52  |            |            |                 |    |
|            | Sip_Bsu_   | DYKVEGVSMNPTFQ  | 40  |            |            |                 |    |
|            | Sip_Tma_   | TMLVPTGSMIPTIQ  | 54  |            |            |                 |    |
|            | Sip_Cpn_   | LYEVPTGSMRPTIL  | 114 |            |            |                 |    |
|            | Sip_Ctr_   | LYEVPTGSMRPTIL  | 119 |            |            |                 |    |
|            |            |                 |     |            |            |                 |    |
| Eucarya    | Imp1_Sce_  | FTETRGESMLPTLS  | 46  |            |            |                 |    |
|            | Imp2_Spo_  | VQMTSGSPSMPTLN  | 41  |            |            |                 |    |
|            | Tpp_Ath_   | PKSIPSTSMYPTLD  | 190 |            |            |                 |    |
|            |            |                 |     |            |            |                 |    |
|            | Consensus  | p ip SM ptl     |     |            |            |                 |    |

FIGURE 5: Conserved box B residues in P-type and ER-type SPases from archaea, eubacteria, and eucarya. These series are generated from ClustalX version 1.8 (29) amino acid alignments of all P-type (A) and ER-type (B) SPases (currently deposited in GenBank) as described by Tjalsma et al. (27) and Dalbey et al. (5). The Ser 88 residue (*E. coli*) is indicated by an asterisk. In the consensus sequence, upper case indicates strictly conserved residues and lower case indicates conserved residues appearing in greater than 50% of the aligned sequences. (A) Alignment of conserved box B residues in P-type SPases. *Eco*, *Escherichia coli*; *Sty*, *Salmonella typhimurium*; *Hin*, *Haemophilus influenzae*; *Pfl*, *Pseudomonas fluorescens*; *Bja*, *Bradyrhizobium japonicum*; *Rca*, *Rhodobacter capsulatus*; *Mle*, *Mycobacterium leprae*; *Mtu*, *Mycobacterium tuberculosis*; *Sli*, *Streptomyces lividans*; *Sco*, *Streptomyces coelicolor*; *Pla*, cyanobacterium *Phormidium laminosum*; *Ssp*, *Synechocystis* sp. strain PCC6803 II; *Aae*, *Aquifex aeolicus*; *Tpa*, *Treponema pallidum*; *Hpy*, *Helicobacter pylori* J99; *Bbu*, *Borrelia burgdorferi*; *Spn*, *Streptococcus pneumoniae*; *Smi*, *Streptococcus mitis*; *Bca*, *Bacillus caldolyticus*; *Sau*, *Staphylococcus aureus*; *Sca*, *Staphylococcus carnosus*; *Bsu*, *Bacillus subtilis*; *Bam*, *Bacillus amyloliquefaciens*; *Bli*, *Bacillus licheniformis*; *Tma*, *Thermotoga maritima*; *Cpn*, *Chlamydia pneumoniae*; *Ctr*, *Chlamydia trachomatis*; *Sce*, *Saccharomyces cerevisiae*; *Ath*, *Arabidopsis thaliana*; *Sip*, signal peptidase; *Spi*, *Streptococcus pneumoniae* signal peptidase I; *Sps*, signal peptidase from *S. aureus*; *Imp*, inner membrane protease; *Tpp*, thylakoidal processing peptidase. (B) Alignment of conserved box B residues in ER-type SPases. *Mth*, *Methanobacterium thermoautotrophicum*; *Mja*, *Methanococcus jannaschii*; *Pho*, *Pyrococcus horikoshii*; *Pab*, *Pyrococcus abyssi*; *Afu*, *Archaeoglobus fulgidus*; *Ape*, *Aeropyrum pernix*; *Bsu*, *Bacillus subtilis*; *Cpe*, *Clostridium perfringens*; *Ath*, thale cress *A. thaliana*; *Sce*, *S. cerevisiae*; *Spo*, *Schizosaccharomyces pombe*; *Rno*, *Rattus norvegicus*; *Mmu*, *Mus musculus*; *Cfa*, *Canis familiaris*; *Hsa*, *Homo sapiens*; *Sip*, signal peptidase; *Sec*, secretory protein; *Spc*, signal peptidase complex.

(25) and of a distal Thr-stabilized interaction in subtilisin BPN' (31) that could be replaced with a Ser residue while maintaining efficient enzymatic activity. This work with *E. coli* SPase I, however, is the first report of a Ser residue involved in the oxyanion hole of the Ser/Lys dyad class and in the serine protease class in general. To our knowledge, no Ser residue has been reported as being involved in oxyanion stabilization in any of the serine or cysteine proteases. Finally, though in the inhibitor-bound crystal structure (8) of truncated *E. coli* SPase I the Ser 88 residue is not in an optimal position for oxyanion stabilization, the

results presented here are consistent with crystallographic data of the recently solved native structure (Paetzl, Dalbey, Strynadka, unpublished results). In the native structure the Ser 88 residue is in the correct position to participate in the oxyanion hole.

#### ACKNOWLEDGMENT

Special thanks go to Don Ordaz at The Ohio State University Department of Microbiology biofermentation facilities and to Roger Granet at CAS for critical reading of the manuscript.

## REFERENCES

1. Date, T. (1983) *J. Bacteriol.* 154, 76–83.
2. Bohni, P. C., Deshaies, R. J., and Schekman, R. W. (1988) *J. Cell Biol.* 106, 1035–1042.
3. Zhang, Y. B., Greenberg, B., and Lacks, S. A. (1997) *Gene* 194, 249–255.
4. Black, M. T., and Bruton, G. (1998) *Curr. Pharm. Des.* 4, 133–154.
5. Dalbey, R. E., Lively, M. O., Bron, S., and van Dijl, J. M. (1997) *Protein Sci.* 6, 1129–1138.
6. Barrett, A. J., Rawlings, N. D., and Woessner, J. F. (1998) *Handbook of proteolytic enzymes*, Academic Press, San Diego, CA.
7. VanValkenburgh, C., Chen, X., Mullins, C., Fang, H., and Green, N. (1999) *J. Biol. Chem.* 274, 11519–11525.
8. Paetzel, M., Dalbey, R. E., and Strynadka, N. C. (1998) *Nature* 396, 186–190.
9. Fersht, A. R., Shi, J. P., Knill-Jones, J., Lowe, D. M., Wilkinson, A. J., Blow, D. M., Brick, P., Carter, P., Waye, M. M., and Winter, G. (1985) *Nature* 314, 235–238.
10. Inada, T., Court, D. L., Ito, K., and Nakamura, Y. (1989) *J. Bacteriol.* 171, 585–587.
11. Klenotic, P. A., Carlos, J. L., Samuelson, J. C., Schuenemann, T. A., Tschantz, W., Paetzel, M., Strynadka, N. C. J., and Dalbey, R. E. (2000) *J. Biol. Chem.* 275, 6490–6498.
12. Sanger, F., Nicklen, S., and Coulson, A. R. (1977) *Proc. Natl. Acad. Sci. U.S.A.* 74, 5463–5467.
13. Cohen, S. N., Chang, A. C., Boyer, H. W., and Helling, R. B. (1973) *Proc. Natl. Acad. Sci. U.S.A.* 70, 3240–3244.
14. Chatterjee, S., Suci, D., Dalbey, R. E., Kahn, P. C., and Inouye, M. (1995) *J. Mol. Biol.* 245, 311–314.
15. Tschantz, W. R., Paetzel, M., Cao, G., Suci, D., Inouye, M., and Dalbey, R. E. (1995) *Biochemistry* 34, 3935–3941.
16. Tschantz, W. R., Sung, M., Delgado-Partin, V. M., and Dalbey, R. E. (1993) *J. Biol. Chem.* 268, 27349–27354.
17. Jones, T. A., Zou, J. Y., Cowan, S. W., and Kjeldgaard (1991) *Acta Crystallogr. A* 47, 110–119.
18. Kim, Y. T., Muramatsu, T., and Takahashi, K. (1995) *Eur. J. Biochem.* 234, 358–362.
19. McDonald, I. K., and Thornton, J. M. (1994) *J. Mol. Biol.* 238, 777–793.
20. Paetzel, M., Strynadka, N. C., Tschantz, W. R., Casareno, R., Bullinger, P. R., and Dalbey, R. E. (1997) *J. Biol. Chem.* 272, 9994–10003.
21. Menard, R., Carriere, J., Laflamme, P., Plouffe, C., Khouri, H. E., Vernet, T., Tessier, D. C., Thomas, D. Y., and Storer, A. C. (1991) *Biochemistry* 30, 8924–8928.
22. Rao, S. N., Singh, U. C., Bash, P. A., and Kollman, P. A. (1987) *Nature* 328, 551–554.
23. Carter, P., and Wells, J. A. (1990) *Proteins: Struct., Funct., Genet.* 7, 335–342.
24. Bryan, P., Pantoliano, M. W., Quill, S. G., Hsiao, H. Y., and Poulos, T. (1986) *Proc. Natl. Acad. Sci. U.S.A.* 83, 3743–3745.
25. Nicolas, A., Egmond, M., Verrips, C. T., de Vlieg, J., Longhi, S., Cambillau, C., and Martinez, C. (1996) *Biochemistry* 35, 398–410.
26. Menard, R., and Storer, A. C. (1992) *Biol. Chem. Hoppe Seyler* 373, 393–400.
27. Tjalsma, H., Bolhuis, A., van Roosmalen, M. L., Wiegert, T., Schumann, W., Broekhuizen, C. P., Quax, W. J., Venema, G., Bron, S., and van Dijl, J. M. (1998) *Genes Dev.* 12, 2318–2331.
28. Jeanmougin, F., Thompson, J. D., Gouy, M., Higgins, D. G., and Gibson, T. J. (1998) *Trends Biochem. Sci.* 23, 403–405.
29. Thompson, J. D., Gibson, T. J., Plewniak, F., Jeanmougin, F., and Higgins, D. G. (1997) *Nucleic Acids Res.* 25, 4876–4882.
30. Saitou, N., and Nei, M. (1987) *Mol. Biol. Evol.* 4, 406–425.
31. Braxton, S., and Wells, J. A. (1991) *J. Biol. Chem.* 266, 11797–11800.
32. Kraulis, P. J. (1991) *J. Appl. Crystallogr.* 24, 945–949.

BI000301L